

Published in final edited form as:

*J Am Chem Soc.* 2010 December 22; 132(50): 17933–17944. doi:10.1021/ja1086485.

## Indolyne Experimental and Computational Studies: Synthetic Applications and Origins of Selectivities of Nucleophilic Additions

G-Yoon J. Im, Sarah M. Bronner, Adam E. Goetz, Robert S. Paton, Paul H.-Y. Cheong, K. N. Houk\*, and Neil K. Garg\*

Department of Chemistry and Biochemistry, University of California, Los Angeles, California 90095

### Abstract

Efficient syntheses of 4,5-, 5,6-, and 6,7-indolyne precursors beginning from commercially available hydroxyindole derivatives are reported. The synthetic routes are versatile and allow access to indolyne precursors that remain unsubstituted on the pyrrole ring. Indolynes can be generated under mild fluoride-mediated conditions, trapped by a variety of nucleophilic reagents, and used to access a number of novel substituted indoles. Nucleophilic addition reactions to indolynes proceed with varying degrees of regioselectivity; distortion energies control regioselectivity and provide a simple model to predict the regioselectivity in the nucleophilic additions to indolynes and other unsymmetrical arynes. This model has led to the design of a substituted 4,5-indolyne that exhibits enhanced nucleophilic regioselectivity.

### Introduction

The indole heterocycle (**1**, Figure 1) is observed in an astonishing number of natural products and medicinal agents.<sup>1,2</sup> More than 10,000 biologically active indole derivatives have been discovered to date, of which over two hundred are currently marketed as pharmaceuticals or are undergoing clinical trials.<sup>3</sup> These include the common chemotherapeutics vincristine, vinorelbine, and vinblastine.<sup>4</sup> Despite the development of an impressive array of strategies to synthesize C2- and C3-functionalized indoles,<sup>5</sup> methods to access benzenoid-substituted indoles remain limited.<sup>1</sup>

Our approach to benzenoid-substituted indoles contrasts with the usual paradigm of indole reactivity. The indole heterocycle is typically exploited for its nucleophilic character (**1**→**2**, Figure 1);<sup>6</sup> however, methods for rendering indoles susceptible to attack by nucleophiles are rare (**1**→**3**).<sup>7</sup> We envisioned that aryne derivatives of indoles, or “indolynes” (e.g., **4–6**), could serve as electrophilic indole surrogates. This umpolung of the indole reactivity would not only be conceptually interesting, but would also provide unconventional strategies to access polysubstituted indoles. Such motifs are often considered medicinally ‘privileged’ and are also observed in countless natural products, such as the complex bioactive alkaloids **7–18** (Figure 2).

houk@chem.ucla.edu; neilgarg@chem.ucla.edu.

Supporting information available. Detailed experimental details and compound characterization data. Comparison of optimizations at different levels of theory, absolute energies, Cartesian coordinates, and full authorship of reference 35. This material is available free of charge via the Internet at <http://pubs.acs.org>.

Whereas arynes have been studied extensively over the past century,<sup>8,9</sup> indole derivatives of arynes have received less attention. Indolynes were first reported in the 1960's by Igolen and co-workers.<sup>10</sup> In a key experiment, it was found that C3-unsubstituted 4,5-indolyne **20** could be generated from 5-bromoindole (**19**) and KNH<sub>2</sub> in ammonia to afford a complex mixture of products, which upon purification, furnished 4- and 5-aminoindole products **21** and **22** (Figure 3). The field of indolyne chemistry lay dormant for over four decades,<sup>11</sup> until our groups and Buszek's laboratory entered the area. In 2007, Buszek's laboratory demonstrated that C3-substituted indolynes could be generated from dihaloindoles in the presence of butyllithium reagents.<sup>12a</sup> The presumed indolyne intermediates were trapped with furan to afford Diels–Alder products (e.g., **23+24**→**26**). Further studies have been reported by Buszek,<sup>12</sup> which include indolyne Diels–Alder reactions of substituted furans and cyclopentadiene, the total synthesis of trikentrin A and herbindole A using an indolyne Diels–Alder reaction, and access to *N*- and C3-substituted indolynes from silyltriflate precursors for use in the furan Diels–Alder reaction.

In this article,<sup>13</sup> we report efficient syntheses of 4,5-, 5,6-, and 6,7-indolyne precursors beginning from commercially available hydroxyindole derivatives. The synthetic routes are versatile, and for the first time, allow access to indolynes that remain unsubstituted at N1, C2, and C3 of the pyrrole ring. Indolynes can be generated under mild fluoride-mediated conditions, trapped by a variety of reagents, and used to access a number of novel substituted indoles. Nucleophilic addition reactions to indolynes proceed with varying degrees of regioselectivity. A computational and experimental study reveals that distortion energies control regioselectivity and provides a simple model for predicting the regioselectivity in the nucleophilic addition to indolynes and unsymmetrical arynes. This model has led to the design of a substituted 4,5-indolyne that exhibits enhanced nucleophilic regioselectivity.

## Results and Discussion

### Synthesis of a 4,5-indolyne precursor and synthetic applications

To initiate studies, 4,5-indolyne **29** was selected as our primary target (Scheme 1). If accessible under mild reaction conditions, indolyne **29** could undergo nucleophilic additions and pericyclic reactions to provide a range of synthetic applications. We elected to utilize Kobayashi's approach to aryne generation<sup>14</sup> and hypothesized that indolyne **29** could be obtained from indolylsilyltriflate precursor **27**. At the time of our studies, routes to indolylsilyltriflates were not known,<sup>15</sup> but could plausibly begin from commercially available hydroxyindole derivatives (e.g., **28**).

The synthesis of an appropriate indolyl silyltriflate proved challenging, primarily because of the acidity of the C2 hydrogen and the electron-rich nature of the indole ring.<sup>16</sup> Nonetheless, extensive experimentation led to the development of an efficient route to silyltriflate **27** (Scheme 2). Commercially available 5-benzyloxyindole (**33**) was converted to hydroxyindole **28** following a known two-step sequence.<sup>17,18</sup> Reaction of hydroxyindole **28** with isopropyl isocyanate, in the presence of catalytic Et<sub>3</sub>N, afforded carbamate **34**. Of note, the conversion of **33** to carbamate **34** proceeds in 85% yield, and requires only one final chromatographic purification. Following the protocol disclosed by Snieckus and Hoppe,<sup>19</sup> carbamate **34** underwent *o*-lithiation/silylation to provide silyl carbamate **35**.<sup>20</sup> Testament to the outstanding *ortho*-directing ability of carbamates,<sup>21</sup> the relatively acidic C2 proton of the *N*-methylindole is not disturbed in this process. Although initial attempts to elaborate silyl carbamate **35** to silyltriflate **27** in a stepwise fashion were met with difficulty,<sup>22</sup> an efficient one-pot deprotection/triflation sequence proved successful. Our optimized route to silyltriflate **27** can be carried out on multigram scale, and proceeds in 63% overall yield. To confirm that silyltriflate **27** would function as a suitable precursor to the targeted 4,5-

indolyne **29**, silyltriflate **27** was reacted with TBAF in the presence of furan (**24**) to afford Diels–Alder product **36** in 85% yield.

A number of heteroatom- and carbon-based nucleophiles undergo smooth reaction with indolyne **29**, which indeed functions as an electrophilic indole surrogate (Table 1). Treatment of silyltriflate **27** with *p*-cresol in the presence of CsF led to the formation of products **37a** and **37b** (entry 1). Similarly, the use of aniline as the nucleophilic trapping agent provided adducts **38a** and **38b** (entry 2),<sup>23</sup> whereas trapping with *p*-methylthiophenol afforded sulfur-containing products **39a** and **39b** (entry 3). With respect to carbon-based nucleophiles, the use of a cyclic  $\beta$ -enaminoketone generated indole products **40a** and **40b** (entry 4).<sup>24</sup> Furthermore, trapping with potassium cyanide afforded cyanoindoles **41a** and **41b** (entry 5). The latter result is notable because cyanide has rarely been used in nucleophilic addition reactions to arynes.<sup>25</sup>

A variety of formal cycloaddition processes involving indolyne **29** were used to access several unique 4,5-disubstituted indole derivatives (Table 2). For instance, reaction of benzylazide and silyltriflate **27**, in the presence of TBAF, provided access to indolyltriazoles **42a** and **42b** in 86% yield, via a formal aryne cycloaddition (entry 1).<sup>26</sup> Moreover, a formal [2+2] cycloaddition provided indolylcyclobutanones **43a** and **43b** (entry 2), whereas a variant involving cycloaddition followed by fragmentation provided ketoesters **44a** and **44b** (entry 3).<sup>27</sup> Of note, each of the examples shown in Tables 1 and 2 reflect an interesting general preference for initial nucleophilic attack at C5 of the presumed 4,5-indolyne intermediate **29** with selectivity as high as 12.5:1 (Table 1, entry 2). An explanation for this observation is presented in the latter part of this manuscript.

Diels–Alder reactions of indolyne **29** were also investigated as a means to access additional 4,5-disubstituted indole products from silyltriflate **27** (Table 3). In addition to furan (see Scheme 2), *N*-Boc-pyrrole and cyclopentadiene could also be used to trap indolyne **29**, thus affording adducts **45** and **46**, respectively (entries 1 and 2). Furthermore, reaction in the presence of  $\alpha$ -pyrone produced benzoindole **47** (entry 3), presumably via a Diels–Alder/retro Diels–Alder process with concomitant loss of CO<sub>2</sub>. Finally, trapping of indolyne **29** with anthracene furnished indolyltriptycene **48** in 72% yield (entry 4).

### Stability and functionalization of indolyne precursors

Our studies (vide supra) show that indolyne methodology can be used to access a range of unique indole derivatives. It should be noted that C3 in all indolyne adducts remains unfunctionalized, and could be easily substituted if so desired. Alternatively, we hypothesized that silyltriflate **27** could be further substituted before indolyne generation and trapping. As shown in Scheme 3, silyltriflate **27** is stable to a range of reaction conditions and can be readily functionalized at C3 through bromination (**27**→**49**),<sup>28</sup> formylation (**27**→**50**),<sup>29</sup> or Lewis acid-mediated acetylation (**27**→**51**).<sup>7d</sup> Furthermore, in each case, the silyltriflate remains intact, allowing for subsequent indolyne generation and trapping. By employing furan (**24**) as a trapping agent, indolyne cycloadducts **52**, **53**, and **54** could be obtained in good yield.

The reaction sequence highlighted in Scheme 4 demonstrates the viability of carrying indolyl silyltriflates through multistep synthesis. 3-Bromo silyltriflate **49** was treated with *t*-BuLi at –78 °C to facilitate halogen-metal exchange. Subsequent quenching with boronate **55** delivered boronic ester **56** in 72% yield.<sup>28</sup> Next, boronic ester **56** underwent Pd-catalyzed Suzuki–Miyaura coupling with iodobenzene at 100 °C to furnish 3-phenyl silyltriflate **57**. It is noteworthy that the silyltriflate functionality withstands both harsh base (i.e., *t*-BuLi) and Pd(0). Treatment of silyltriflate **57** with CsF in the presence of furan (**24**) provided adduct

**26** in 70% yield, thus demonstrating that silyltriflate **57** serves as an efficient precursor to indolyne **25**.

### Generation and trapping of 5,6- and 6,7-indolynes

Our strategy for preparing indolyl silyltriflates from hydroxyindole precursors proved amenable to the synthesis of 5,6- and 6,7-indolyne precursors. The synthesis of 5,6-indolyne precursor **59** is depicted in Scheme 5. As described earlier, *o*-lithiation/silylation of carbamate **34** afforded C4-silylated indole **35** in 84% yield, which could be elaborated to 4,5-indolyne precursor **27** (see Scheme 2). However, the C6-silylated indole **58** also formed in this process in 10% yield. Carbamate cleavage, followed by stirring with PhNTf<sub>2</sub>, provided silyltriflate **59** in 70% yield. The overall route to **59**, although low-yielding, enabled our early studies of 5,6-indolynes. Higher yielding routes to 5,6-indolyne precursors were later developed (vide infra).

A suitable silyltriflate precursor to a 6,7-indolyne proved most difficult to access. Exploratory efforts beginning from 7-hydroxyindole derivatives failed. For example, 7-benzyloxyindole **60** was elaborated to carbamate **61** using our standard two-step sequence (Scheme 6). Attempts to effect the *o*-lithiation/silylation of carbamate **61** led to competitive C2 lithiation and decomposition products, rather than to the desired silylcarbamate **62**. Thus, silyltriflate **63** was inaccessible.

Unsuccessful efforts to synthesize silyltriflate **63** (see Scheme 6) led us to pursue the synthesis of regioisomeric silyltriflate **68** (Scheme 7). Readily available 6-benzyloxyindole **64** was smoothly converted to carbamate **65** in 77% yield. Subsequent treatment of carbamate **65** with TBSOTf and TMEDA, followed by *n*-BuLi, led primarily to C7 lithiation.<sup>30</sup> Quenching with TMSCl delivered silylcarbamate **66**. Although our previously described protocol for elaborating aryl carbamates to aryl triflates led primarily to hydroxyindole **67**,<sup>31</sup> a modified procedure using *n*-BuLi in place of DBU furnished silyltriflate **68** in 91% yield.

To confirm that silyltriflates **59** and **68** serve as efficient indolyne precursors, each compound was independently subjected to furan (**24**) in the presence of fluoride sources (Figure 4). Trapping of 5,6-indolyne **69** delivered adduct **70** in 92% yield. Similarly, 6,7-indolyne **71** underwent [4+2] cycloaddition to provide adduct **72** in 95% yield. Nucleophilic additions and formal cycloadditions of indolynes **69** and **71** were also carried out and, as will be described below, found to proceed efficiently and with interesting regioselectivities.

### Indolyne precursors with alternative *N*-substituents

Having discovered that indolynes can be generated under mild fluoride-mediated conditions and serve as building blocks for the synthesis of polysubstituted indoles, we synthesized indolyne precursors with alternative *N*-substituents. Indolyl silyltriflates with removable groups, such as Boc and TIPS, were pursued, in addition to *N*-unsubstituted silyltriflates. Syntheses of the targeted indolyne precursors in the 4,5-indolyne series are shown in Scheme 8, and parallel our synthesis of 4,5-indolyne precursor **27** (see Scheme 2). Beginning with TIPS-protection of 5-benzyloxyindole (**33**), *N*-TIPS-silyltriflate **76** was prepared in 85% yield over five steps. *N*-TIPS-silyltriflate **76** served as the precursor to the corresponding *N*-H and *N*-Boc compounds **77** and **78**, respectively. Of note, when treated with CsF in the presence of furan (**24**), both substrates **76** and **77** are converted to the identical unprotected bicycle **80**, likely via *N*-H indolyne intermediate **79**.<sup>32</sup> Free *N*-H indolynes of the type **79** have never been synthesized previously, but provide a valuable synthetic tool for the synthesis of unprotected, benzenoid-substituted indoles.

As described earlier, our synthesis of an *N*-methyl-5,6-indolyne precursor proceeded in low yield (see Scheme 5). To address this limitation and access 5,6-indolyne precursors with alternative *N*-substituents, we considered the strategies depicted in Scheme 9. Indolyne **5** could be derived from either regioisomeric silyltriflates **81** or **82**, which in turn, would be derived from 5- or 6-substituted precursors **83** or **86**, respectively. Since the 5-substituted carbamate was observed to favor formation of the 4,5-substituted species **84** over the desired 5,6-substituted product **85**, we explored the use of 6-carbamylated substrates. Although C7 lithiation of **86** was favored when R=Me, it was hypothesized that the use of a bulky TIPS protective group would disfavor C7 lithiation, ultimately allowing access to 5-silylated product **88**.

The execution of this approach to 5,6-indolynes is shown in Scheme 10. Commercially available 6-benzyloxyindole (**89**) was TIPS-protected under standard conditions. Conversion of **90** to carbamate **91** proceeded in 82% yield using our robust two-step sequence. In the key *o*-lithiation/silylation experiment, functionalization of **91** occurred exclusively at C5 to deliver silylcarbamate **92**. Analogous to previous studies, carbamate **92** was elaborated to *N*-TIPS silyltriflate **93**, which in turn, was readily converted to *N*-H and *N*-Boc silyltriflates **94** and **95**, respectively.

The synthesis of 6,7-indolyne precursors with variable *N*-substituents proved challenging. Nevertheless, two routes were developed beginning from 6-hydroxyindole derivatives. The first generation approach is shown in Scheme 11. Boc-protection of benzyloxyindole **89**, followed by treatment with H<sub>2</sub> and Pd/C furnished a hydroxyindoline intermediate. Subsequent reaction with *i*-PrNCO in the presence of Et<sub>3</sub>N furnished carbamate **96**. *o*-Lithiation/silylation of carbamate **96** delivered 6,7-disubstituted indoline **97**, albeit with competitive functionalization at C5.<sup>33</sup> Nonetheless, DDQ oxidation furnished indole **98**, which was readily converted to silyltriflate **99**. The *N*-Boc group of **99** was removed by thermolysis to provide *N*-H indolyne precursor **100**.

A higher yielding route to *N*-H indolyne **100** is depicted in Scheme 12. *O*-silylation and *N*-allylation of 6-hydroxyindole (**101**) afforded protected indole **102**. Subsequent elaboration of TBS ether **102** to carbamate **103** proceeded without event. Lithiation of carbamate **103**, followed by quenching with TMSOTf, furnished silylcarbamate **104** in 78% yield. After installing the silyltriflate (**104**→**105**), the *N*-allyl group was removed<sup>34</sup> to deliver *N*-H silyltriflate **100**.

### Regioselectivity in nucleophilic additions to indolynes

Our studies demonstrate that nucleophilic additions to 4,5-indolynes can occur with significant regioselectivity. A combination of experimental and computational studies was undertaken to determine the origin of these observations. Quantum chemical calculations were performed using Gaussian.<sup>35</sup> The arynes and their transition structures for nucleophilic addition were optimized with B3LYP36 and M06-2X37 hybrid density functionals employing 6-31G(d) or 6-311+G(d,p) basis sets. In addition, optimizations were performed with the B2PLYP double hybrid functional<sup>38</sup> and with MP2 perturbation theory<sup>39</sup> using a 6-31G(d) basis set. All density functional calculations used a fine grid for numerical integration. Solvation effects were evaluated through single point calculations using an implicit CPCM model of acetonitrile,<sup>40</sup> defining the solute surface by UAKS radii.<sup>41</sup> In the manuscript we discuss the results of the B3LYP/6-31G(d) calculations, although optimizations at B3LYP/6-311+G(d,p) and M06-2X/6-311+G(d,p) levels of theory (see Supporting Information) give very similar aryne geometries and also predict the same sense of regioselectivity in each case studied.

The results of several nucleophilic additions to 4,5-indolyne **29** are shown in Table 4, in addition to the results of density functional computations performed at the B3LYP/6-31G(d) level of theory. The experimental preference for attack at C5 was matched well by the activation free energies of the competing transition structures for each of the nucleophiles we studied, while the magnitudes are usually exaggerated. Activation barriers are very low, in some cases zero, so that variational effects and dynamics may cause selectivities to be less than predicted by  $\Delta\Delta G^\ddagger$ . Cyanide addition has no energetic barrier, but approach of the nucleophile at C5 is favored over C4 for all distances.<sup>42</sup> The major indolotriazole adduct formed from azide cycloaddition involves attack at C5 by the nucleophilic internal nitrogen. Ion pairing and entropic effects should cause these reactions to have positive barriers.

Figures 5 and 6, respectively, show the calculated structures of 4,5-indolyne **29** and transition state (TS) geometries for nucleophilic addition of aniline, *p*-cresol and methylazide (as a model for benzylazide used in experiment). For each of the nucleophiles, the bond angle of the terminus of the aryne that undergoes attack is flattened in the transition structure, whereas the angle at the other terminus is compressed. This picture can be understood in terms of the polarization of the C≡C bond, with developing positive charge at the site of attack and negative charge at the adjacent carbon. We have also found that the computed distortion energies,  $\Delta E_d^\ddagger$ , are useful in quantifying the transition state stabilities. These distortion energies (also termed deformation energy<sup>43</sup> or activation strain<sup>44</sup>) are defined as the energies required to distort the indolyne and nucleophile into their TS geometries without interaction between them. These are shown in Figure 6. Computed distortion energies have been shown to correlate well with activation barriers in a number of bimolecular reactions: 1,3-dipolar cycloadditions,<sup>45</sup> 1,4-dihydrogenations, Diels–Alder cycloadditions<sup>46</sup> and cycloadditions involving fullerenes and nanotubes.<sup>47</sup> While this is the first time that distortion energies have been used to understand regioselectivities of additions to arynes,<sup>13b</sup> one of us previously explored the LUMO-lowering effect of bending distortions on alkynes and benzyne that leads to their greater reactivity towards nucleophiles over electrophiles.<sup>48</sup>

Internal angles of 4,5-indolyne **29** show that the aryne is distorted, particularly at C3a ( $\theta_{\text{CCC}} = 110^\circ$  vs.  $\theta_{\text{HCC}} = 126^\circ$  in pyrrole). Nucleophilic attack at C5 relieves some of the strain at C3a (e.g., opening from 110 to 118° in **TS-1**), but attack at C4 adds to the unfavorable distortion at C3a (e.g., closing from 110 to 108° in **TS-2**). Attack at C4 has 1.4 kcal/mol greater distortion energy than at C5 due to compression at C3a, leading to a lower activation barrier.

The types of distortions present in the indolyne TSs shown in Figure 6 can be understood from the geometry for nucleophilic attack on benzyne (**106**). As shown in Figure 7, benzyne is flattened at the point of attack of aniline in **TS-7** ( $\theta_{\text{CCC}} = 136^\circ$ ), giving the orbital at the site of attack significant p-character and a slight positive charge, while the adjacent angle is compressed ( $\theta_{\text{CCC}} = 113^\circ$ ) increasing s-character to stabilize the developing carbanion (see **TS-8**). We reasoned that nucleophilic addition to unsymmetrical arynes (e.g., indolynes) is favored for attack at the carbon that requires minimal geometrical and energetic change from aryne to TS structure. This is the carbon at which the internal angle is larger, as it is in the nucleophilic addition transition state. In the structure of 4,5-indolyne (see Figure 5), C5 is flatter than C4 (129° vs. 124°) and accordingly, nucleophilic addition is preferred at C5.

Regioselectivities of nucleophilic attack on 5,6- and 6,7-indolynes were studied computationally prior to experiment. There is uniformly lower unsymmetrical distortion and lower addition selectivity in nucleophilic attack on 5,6-indolyne seen in the results of our calculations and also in experiment (Table 5). Figure 8 shows the computed structures of 5,6-indolyne **69** and the TSs for nucleophilic addition. The slightly greater flattening of **69** at

C5 than at C6 (internal angles are 130° and 127° respectively) can be attributed to electron withdrawal by the indole nitrogen (the charges at C5 and C6 are -0.01 and -0.03e, respectively). This facilitates attack at C5 in **TS-10**, **TS-12**, and **TS-14**, albeit to only a small extent, paralleling the reactivity depicted in **TS-9**.

In contrast to the 5,6-indolyne, the computed internal angles at the C≡C termini of 6,7-indolyne **71** are very different from each other with  $\theta_{\text{CCC}} = 135$  and 117° (Figure 9). Since the flatter of the two termini is more susceptible to nucleophilic attack, we expected that the 6,7-indolyne would display a high regiochemical preference for addition to C6. Nucleophilic attack on 6,7-indolyne at C6 is highly favored because of the smaller distortion energy, as the indolyne is already distorted into the TS geometry.<sup>49</sup> In fact, the structure of 6,7-indolyne is practically identical to that of the TS for aniline addition to benzyne (see Figure 7, **TS-7**). There is no calculated energetic barrier for the attack at C6 by aniline, while C7 attack (**TS-12**) has a  $\Delta E_d$  of 8.8 kcal/mol, which is higher than that for any other of the TSs computed for the indolyne isomers. These results are in accord with the greater selectivity for C6 attack shown here. Extremely high levels of regioselectivity are observed experimentally (Table 6), and even azide cycloaddition gives very high selectivity. The 6,7-indolynes also display remarkably high regioselectivity in cycloadditions with 2-substituted furans, unlike 4,5- and 5,6-indolynes.<sup>12e</sup> Complementary to our rationalization based on the distortion energies required to achieve the transition state geometry, Buszek and Cramer have also shown that regioselectivity of additions of electron-rich furans to indolynes are influenced by the computed polarization of the C≡C bond.<sup>12e</sup> This polarization is related to the unsymmetrical bending distortions of the indolyne.

### A model for predicting regioselectivity in the nucleophilic addition to indolynes and unsymmetrical arynes

These studies show that computed atomic charges at the triple bond termini are related to the asymmetric distortion of indolynes. Based on this, a distortion model for regioselective nucleophilic addition to fused arynes is depicted in Figure 10. Regioselectivity is controlled by the relative ease of distorting the aryne into the two possible transition structures shown. Unsymmetrical distortion is already present in ring-fused arynes and electron-withdrawing groups (X) can further enhance this distortion by polarizing the aryne. The unsymmetrical distortion biases nucleophilic attack to the flatter, more electropositive end of the aryne, leading to an energetically favorable decrease in ring distortion.

Furthermore, we advocate a comparison of computed internal angles in indolynes as a rapid and reliable method to predict nucleophilic regioselectivity. As exemplified in Figure 11, this predictive tool holds for other unsymmetrical arynes with fused rings,<sup>50-51</sup> in addition to arynes with adjacent polar substituents.<sup>52</sup> In all cases, the terminus of the aryne that is flatter, or more distorted, correlates to the experimentally favored site of nucleophilic attack. The difference in internal angles also relates to the degree of regioselectivity, with higher selectivity observed in the addition to arynes that possess large differences between internal angles. If angle differences are small (4° or less), regioselectivity may be modest or somewhat variable. This predictive model functions at various different levels of theory, where the angles are essentially the same as in these cases.

### Influence of N-substituents on the regioselectivity of indolyne reactions

With a predictive model for determining the regioselectivity in nucleophilic additions to indolynes, we examined the role of substituents on the presumed indolyne intermediates. Figure 12 shows the results of B3LYP/6-31G(d) geometry optimization on 4,5-, 5,6-, and 6,7-indolynes as a function of the nitrogen substituent. Computed geometries for the *N*-H indolynes and *N*-Me indolynes are very similar, indicating that their regioselectivities would

also be very similar. Effects of Boc protection on the indolyne geometry were more noticeable: *N*-Boc-4,5-indolyne is slightly more distorted than the *N*-H and *N*-Me structures, while 5,6- and 6,7-indolynes were slightly less distorted. Although some minor perturbations are observed, these computational results suggest that regioselectivity in nucleophilic additions to each indolyne would not vary significantly by changing the *N*-substituent from methyl to H or Boc.

As described earlier, our robust route to indolyl silyltriflates provided access to a variety of indolyne precursors with differing *N*-substituents. By employing these indolyne precursors in nucleophilic additions and formal cycloaddition reactions, we verified our computational predictions. Experimental results for the 4,5-, 5,6-, and 6,7-indolynes are shown in Tables 7, 8, and 9, respectively. As expected, only minor variations in regioselectivity were observed in all cases. It should be noted that in all reactions involving the *N*-H-6,7-indolyne (Table 9), products indicative of initial attack at C7 were also observed. Although it is not possible to significantly improve regioselectivities based on the *N*-substituent, these studies validate our predictive regioselectivity model and demonstrate that an array of indolyl silyltriflates can be used as building blocks for the synthesis of substituted indoles.

### Influence of a C3 halide substituent on the regioselectivities of 4,5-indolyne reactions

As a means to further probe our predictive regioselectivity model and ultimately improve regioselectivities, the influence of C3 halide substituents on 4,5-indolynes was evaluated. The results of geometry optimization (B3LYP/6-31G(d) for all atoms except Br, for which the Hay–Wadt LANL2DZ effective core potential<sup>53</sup> was used) for 3-bromo-4,5-indolyne **107** are shown in Figure 13. The internal angles at C5 and C4 were found to be 131° and 124°, respectively. This finding suggests that bromoindolyne **107** should display a greater preference for nucleophilic attack at C5 compared to its C3-unsubstituted derivative (for comparison, the desbromo derivative of **107** possesses internal angles of 129° and 125°; see Figure 5).

Our computational prediction was tested experimentally by the reaction of 3-bromosilyltriflate **49** (see Scheme 3 for preparation) with benzylazide in the presence of CsF (Scheme 13). Adduct **108a** was the major product obtained, showing that initial attack of the presumed indolyne intermediate **107** is favored at C5. Of note, the degree of regioselectivity was higher compared to that seen for the corresponding desbromo species (6.8:1 versus 2.4:1), consistent with our calculations. Analogous results were obtained in the nucleophilic addition of cyanide.<sup>54</sup> The fact that a bromo-substituent could lead to improvements in regioselectivity is significant since the C3 bromide is easy to introduce. Moreover, after the necessary indolyne reaction, the bromide substituent could either be removed reductively or used as a handle for the installation of other functional groups.

### Conclusion

In summary, we have developed an efficient method for accessing a variety of indole derivatives that bear functional groups on the benzenoid ring. Our strategy relies on the generation of indolynes, which act as electrophilic indole surrogates, thus opposing the typical mode of indole reactivity. A series of 4,5-, 5,6-, and 6,7-indolynes are accessible from indolylsilyltriflate precursors and can be readily employed in both nucleophilic additions and formal cycloaddition processes. Varying degrees of regioselectivity are observed, and we have shown that these regioselectivities are controlled by distortion energies. These studies have led to the discovery of a simple model to predict the regioselectivity in the nucleophilic additions to indolynes and other unsymmetrical arynes. Applications of indolyne methodology in the synthesis of complex molecules are currently being explored in our laboratories.



## Supplementary Material

Refer to Web version on PubMed Central for supplementary material.

## Acknowledgments

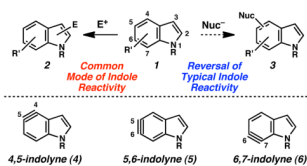
We are grateful to the National Science Foundation (CHE-0548209 to K.N.H. and CHE-0955864 to N.K.G.) and the National Institute of General Medical Sciences, National Institutes of Health Grant (GM-36700 to K.N.H.), Dupont (N.K.G.), Boehringer Ingelheim (N.K.G.), the Foote Fellowship (S.M.B.), the Fulbright Commission, AstraZeneca and the Royal Commission for 1851 (R.S.P) for financial support.

## References

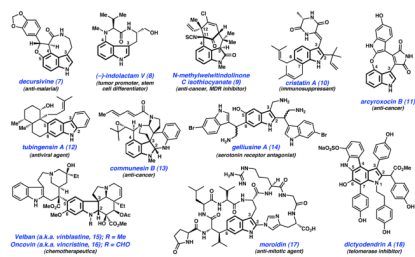
1. a) Sundberg, R.J. *The Chemistry of Indoles*. Academic Press; New York: 1970. b) Sundberg, R.J. *Pyrroles and Their Benzoderivatives: Synthesis and Applications*. In: Katritzky, AR.; Rees, CW., editors. *Comprehensive Heterocyclic Chemistry*. Vol. 4. Pergamon Press; Oxford: 1984. p. 313-376. c) Sundberg, R.J. *Indoles (Best Synthetic Methods)*. Academic Press; New York: 1996. p. 7-11. d) Joule, JA. *Indole and its Derivatives*. In: Thomas, EJ., editor. *Science of Synthesis: Houben-Weyl Methods of Molecular Transformations*. Vol. 10 Chapter 10.13. George Thieme Verlag; Stuttgart: 2000. Category 2
2. a) Horton DA, Bourne GT, Smyth ML. *Chem Rev*. 2003; 103:893–930. [PubMed: 12630855] b) Rodrigues de Sa Alves F, Barreiro EJ, Fraga CAM. *Mini-Rev Med Chem*. 2009; 9:782–793. [PubMed: 19519503]
3. MDL Drug Data Report. MDL Information Systems Inc; San Leandro, CA:
4. a) Kidwai M, Venkataramanan R, Mohan R, Sapra P. *Curr Med Chem*. 2002; 9:1209–1228. [PubMed: 12052173] b) Guerite, F.; Fahy, J. *The Vinca Alkaloids*. In: Cragg, GM.; Kingston, DGI.; Newman, DJ., editors. *Anticancer Agents from Natural Products*. CRCC Press LLC; Boca Raton: 2005. p. 123-135. c) American Cancer Society *Chemotherapy Principles*. [accessed October 10, 2009]. [http://www.cancer.org/docroot/eto/eto\\_1\\_3\\_chemotherapy\\_principles.asp](http://www.cancer.org/docroot/eto/eto_1_3_chemotherapy_principles.asp)
5. For a recent review, see: Bandini M, Eichholzer A. *Angew Chem Int Ed*. 2009; 48:9608–9644.
6. For the nucleophilicity of N-methylindole, see: Mayr H, Kempf B, Ofial AR. *Acc Chem Res*. 2003; 36:66–77. [PubMed: 12534306]
7. For the activation of indoles with stoichiometric chromium, see: a) Semmelhack MF, Rhee H. *Tetrahedron Lett*. 1993; 34:1399–1402. b) Semmelhack MF, Knochel P, Singleton T. *Tetrahedron Lett*. 1993; 34:5051–5054. c) Semmelhack MF, Wulff W, Garcia JL. *J Organomet Chem*. 1982; 240:C5–C10. For an example of Pd-catalyzed arylation in complex molecule synthesis, see: d) MacKay JA, Bishop RL, Rawal VH. *Org Lett*. 2005; 7:3421–3424. [PubMed: 16048307]
8. For reviews, see: a) Pellissier H, Santelli M. *Tetrahedron*. 2003; 59:701–730. b) Wenk HH, Winkler M, Sander W. *Angew Chem Int Ed*. 2003; 42:502–528. c) Sanz R. *Org Prep Proced Int*. 2008; 40:217–291.
9. For reviews regarding heteroaromatic arynes, see: a) Reinecke MG. *Tetrahedron*. 1982; 38:427–498. b) Kauffmann T, Wirthwein R. *Angew Chem Int Ed*. 1971; 10:20–33.
10. a) Julia M, Huang Y, Igolen J. *C R Acad Sci, Ser C*. 1967; 265:110–112. b) Igolen J, Kolb A. *C R Acad Sci, Ser C*. 1969; 269:54–56. For related studies, see: c) Julia M, Goffic FL, Igolen J, Baillarge M. *C R Acad Sci, Ser C*. 1967; 264:118–120. d) Julia M, Igolen J, Kolb M. *C R Acad Sci, Ser C*. 1971; 273:1776–1777.
11. Attempts to synthesize 2,3-indolynes were put forth, but were not successful; see: a) Muller, H. *Dissertation*. University of Heidelberg; 1964. b) Hoffman, RW. *Dehydrobenzene and Cycloalkynes*. Academic Press; New York: 1967. c) Conway SC, Gribble GW. *Heterocycles*. 1992; 34:2095–2108.
12. a) Buszek KR, Luo D, Kondrashov M, Brown N, VanderVelde D. *Org Lett*. 2007; 9:4135–4137. [PubMed: 17880092] b) Brown N, Luo D, VanderVelde D, Yang S, Brassfield A, Buszek KR. *Tetrahedron Lett*. 2009; 50:63–65. c) Buszek KR, Brown N, Luo D. *Org Lett*. 2009; 11:201–204. [PubMed: 19055375] d) Brown N, Luo D, Decapo JA, Buszek KR. *Tetrahedron Lett*. 2009;

- 50:7113–7115. [PubMed: 20877442] e) Garr AN, Luo D, Brown N, Cramer CJ, Buszek KR, VanderVelde D. *Org Lett.* 2010; 12:96–99. [PubMed: 19961152]
13. For preliminary communications involving this work, see: a) Bronner SM, Bahnck KB, Garg NK. *Org Lett.* 2009; 11:1007–1010. [PubMed: 19178159] b) Cheong PHY, Paton RS, Bronner SM, Im GY, Garg NK, Houk KN. *J Am Chem Soc.* 2010; 132:1267–1269. [PubMed: 20058924]
14. Himeshima Y, Sonoda Y, Kobayashi H. *Chem Lett.* 1983:1211–1214.
15. Subsequently, Buszek has reported routes to *N*-Me-C3-phenyl-substituted indolylsilyltriflates using a Fischer indolization strategy; see reference 12b.
16. The electron-rich indole was prone to undesired reactions at C3 and protodesilylation at C4.
17. a) Stadlwieser JF, Dambaur ME. *Helv Chim Acta.* 2006; 89:936–946. b) Gwaltney SL, Imade HM, Barr KJ, Li Q, Gehrke L, Credo RB, Warner RB, Lee JY, Kovar P, Wang J, Nukkala MA, Zielinski NA, Frost D, Ng SC, Sham HL. *Bioorg Med Chem Lett.* 2001; 11:871–874. [PubMed: 11294380]
18. 5-Hydroxyindoles can also be readily prepared by the classic Nenitzescu indole synthesis; for a review, see: Allen GR. *Org React.* 1973; 20:337–454.
19. a) Kauch M, Snieckus V, Hoppe D. *J Org Chem.* 2005; 70:7149–7158. [PubMed: 16122233] b) Kauch M, Hoppe D. *Synthesis.* 2006:1578–1589.
20. For the selective C4 lithiation of a related *N*-silylated substrate, see: Griffen EJ, Roe DG, Snieckus V. *J Org Chem.* 1995; 60:1484–1485.
21. Snieckus V. *Chem Rev.* 1990; 90:879–933.
22. Cleavage of the carbamate of **35** was routinely accompanied by loss of the C4 silyl substituent under a variety of reaction conditions.
23. Liu Z, Larock RC. *J Org Chem.* 2006; 71:3198–3209. [PubMed: 16599619]
24. Ramtohl YK, Chartrand A. *Org Lett.* 2007; 9:1029–1032. [PubMed: 17309270]
25. Scardiglia F, Roberts JD. *Tetrahedron.* 1958; 3:197–208.
26. a) Shi F, Waldo JP, Chen Y, Larock RC. *Org Lett.* 2008; 10:2409–2412. [PubMed: 18476707] b) Campbell-Verduyn L, Elsinga PH, Mirfeizi L, Dierckx RA, Feringa BL. *Org Biomol Chem.* 2008; 6:3461–3463. [PubMed: 19082144]
27. Tambar UK, Stoltz BM. *J Am Chem Soc.* 2005; 127:5340–5341. [PubMed: 15826170]
28. Garg NK, Sarpong R, Stoltz BM. *J Am Chem Soc.* 2002; 124:13179–13184. [PubMed: 12405846]
29. Vilsmeier A, Haack A. *Ber.* 1927; 60:119–122.
30. Quenching of the presumed carbanion with MeOD led to complete deuterium incorporation at C7.
31. The intermediate silyl alcohol readily undergoes protodesilylation by DBU-H<sup>+</sup>.
32. Removal of the *N*-TIPS of **76** occurs more readily than indolyne formation.
33. Attempts to lithiate the corresponding indole led to competitive C2 functionalization.
34. For ruthenium-mediated olefin isomerization, see: a) Kamijo S, Huo Z, Jin T, Kanazawa C, Yamamoto Y. *J Org Chem.* 2005; 70:6389–6397. [PubMed: 16050701] For oxidative cleavage, see: b) Alcaide B, Imendros P, Alonso JM. *Tetrahedron Lett.* 2003; 44:8693–8695. c) Alcaide B, Almendros P, Alonso JM. *Chem Eur J.* 2006; 12:2874–2879. For Et<sub>3</sub>N-promoted *N*-deformylation, see: d) Aizpurua JM, Cossío FP, Lecea B, Palomo C. *Tetrahedron Lett.* 1986; 27:4359–4362.
35. Frisch, MJ., et al. Gaussian 03, revision C.02. Gaussian, Inc; Wallingford, CT: 2004.
36. a) Becke AD. *J Chem Phys.* 1993; 98:5648–5652. b) Lee C, Yang W, Parr RG. *Phys Rev B.* 1988; 37:785–789. c) Vosko SH, Wilk L, Nusair M. *Can J Phys.* 1980; 58:1200–1211. d) Stephens PJ, Devlin FJ, Chabalowski CF, Frisch MJ. *J Phys Chem.* 1994; 98:11623–11627.
37. Zhao Y, Truhlar DG. *Theor Chem Acc.* 2008; 120:215–241.
38. Grimme S. *J Chem Phys.* 2006; 124:034108-1–034108-16. [PubMed: 16438568]
39. Head-Gordon M, Pople JA, Frisch MJ. *Chem Phys Lett.* 1988; 153:503–506.
40. a) Barone V, Cossi M. *J Phys Chem A.* 1998; 102:1995–2001. b) Cossi M, Rega N, Scalmani G, Barone V. *J Comp Chem.* 2003; 24:669–681. [PubMed: 12666158]
41. Takano Y, Houk KN. *J Chem Theory Comput.* 2005; 1:70–77.
42. See Supporting Information for details.
43. Morokuma K. *J Chem Phys.* 1971; 55:1236–1244.

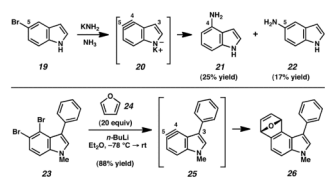
44. Bickelhaupt FM. *J Comput Chem.* 1999; 20:114–128.
45. a) Ess DH, Houk KN. *J Am Chem Soc.* 2007; 129:10646–10647. [PubMed: 17685614] b) Ess DH, Houk KN. *J Am Chem Soc.* 2008; 130:10187–10198. [PubMed: 18613669]
46. Hayden AE, Houk KN. *J Am Chem Soc.* 2009; 131:4084–4089. [PubMed: 19256544]
47. Osuna S, Houk KN. *Chem Eur J.* 2009; 15:13219–13231.
48. a) Strozier RW, Caramella P, Houk KN. *J Am Chem Soc.* 1979; 101:1340–1342. b) Rondan NG, Domelsmith LN, Houk KN, Bowne AT, Levin RH. *Tetrahedron Lett.* 1979; 35:3237–3240.
49. The nucleophilic attack of *p*-cresol on indolynes is accompanied by proton transfer, and the transition states appear to be 4-center reactions, since the proton transfer will occur without a barrier upon nucleophilic attack of the oxygen.
50. For experimental studies of naphthalene, see: a) Kauffmann K, Fischer H, Nürnberg R, Withwein R. *Justus Liebigs Ann Chem.* 1970; 731:23–26. b) Kolomeitsev AA, Vorobyev M, Gillandt H. *Tetrahedron Lett.* 2008; 49:449–454.
51. For studies pertaining to benzyne, see: Hamura T, Ibusuki Y, Sato K, Matsumoto T, Osamura Y, Suzuki K. *Org Lett.* 2003; 5:3551–3554. [PubMed: 14507170]
52. For an experimental study involving 3-methoxybenzyne, see: Yoshida H, Fukushima H, Ohshita J, Kunai A. *J Am Chem Soc.* 2006; 128:11040–11041. [PubMed: 16925418] see also reference 8.
53. Hay PJ, Wadt WR. *J Chem Phys.* 1985; 82:299–310.
54. Trapping of indolyne **107** with cyanide led to a 6.5:1 mixture of products, favoring attack at C5 over C4. This result reflects a notable improvement in regioselectivity compared to that seen in the reaction of the parent desbromo compound with cyanide (3.3:1 selectivity, see Table 1).



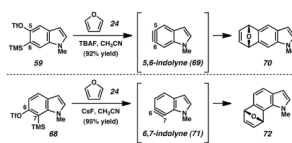
**Figure 1.**  
Indole Reactivity and Indolyne Targets **4–6**.



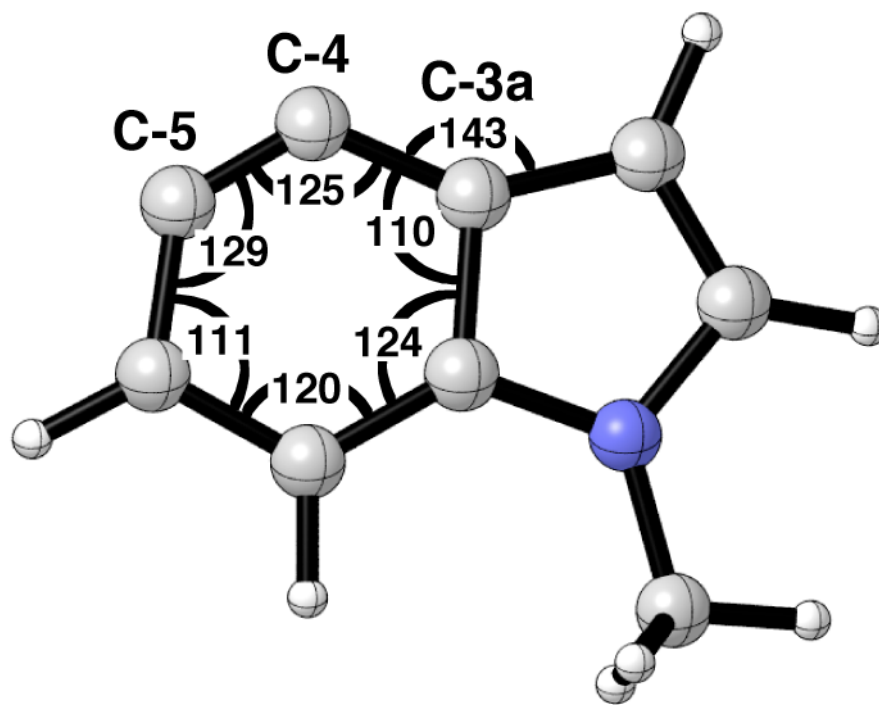
**Figure 2.**  
Benzenoid-substituted indole natural products **7–18**.



**Figure 3.**  
Previous Indolyne Studies.



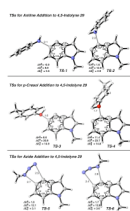
**Figure 4.**  
Generation and trapping of 5,6- and 6,7-indolynes **69** and **71**.



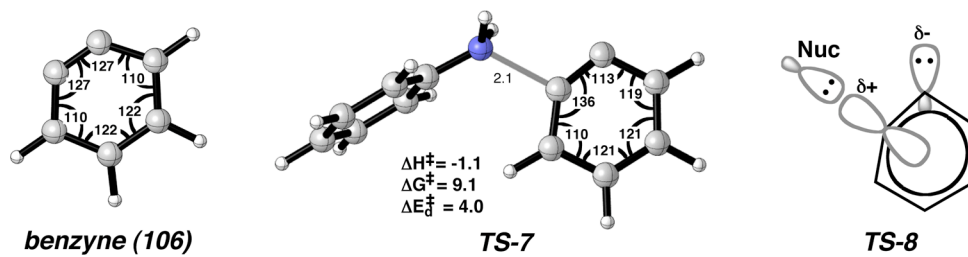
## ***4,5-indolyne (29)***

**Figure 5.**  
B3LYP/6-31G(d) optimized structure of 4,5-indolyne **29**.

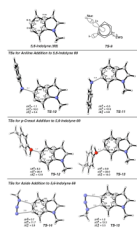




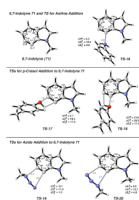
**Figure 6.** B3LYP/6-31G(d) optimized TSs for addition of aniline, *p*-cresol, and methyl azide to indolyne **29**. Energies in kcal/mol.



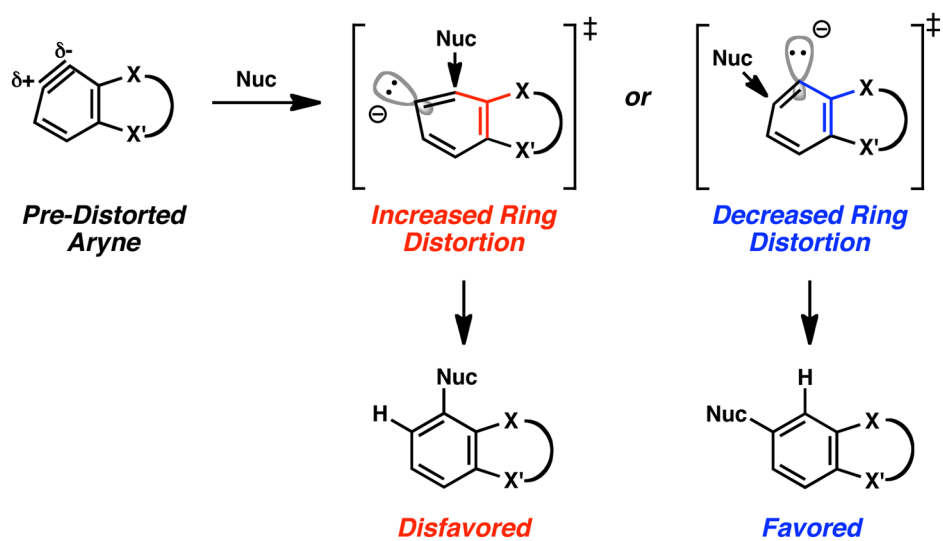
**Figure 7.** B3LYP/6-31G(d) optimized benzyne (**106**) and TS for aniline addition. Energies in kcal/mol.



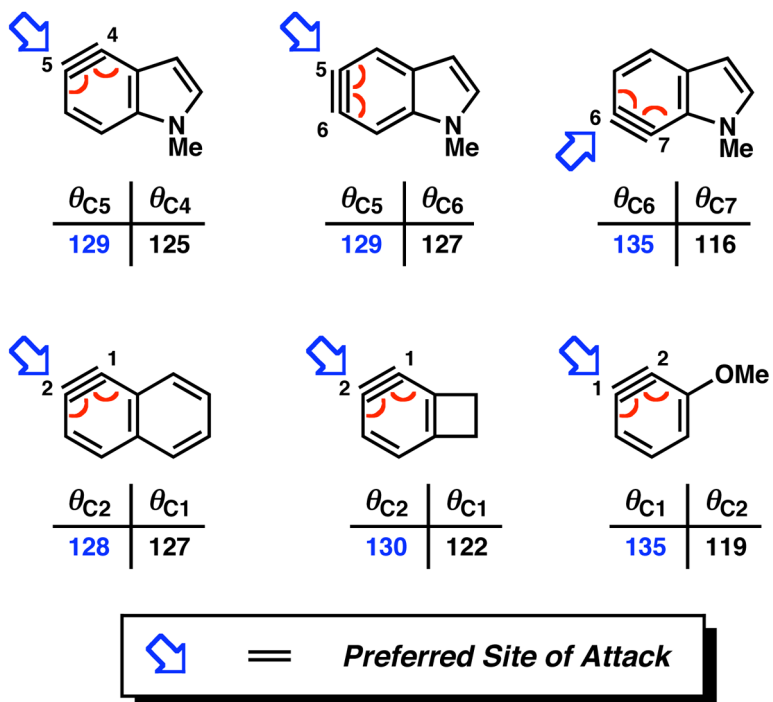
**Figure 8.** B3LYP/6-31G(d) optimized 5,6-indolyne **69** and TSs for aniline addition. Energies in kcal/mol.



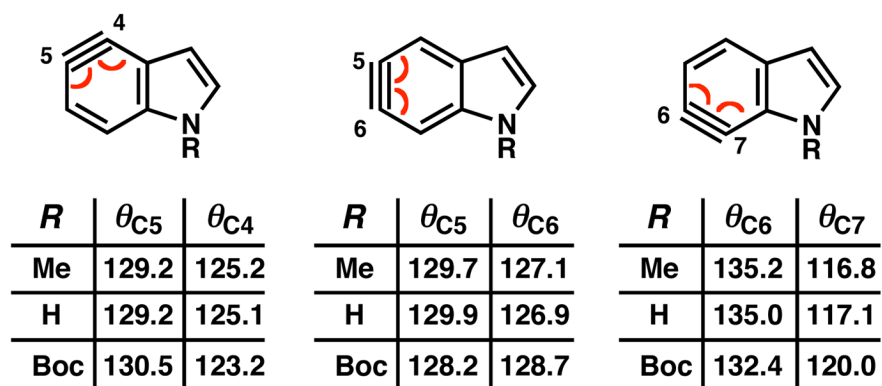
**Figure 9.** B3LYP/6-31G(d) optimized 6,7-indolyne **71** and TSs for aniline, *p*-cresol, and methylazide addition. Energies in kcal/mol.



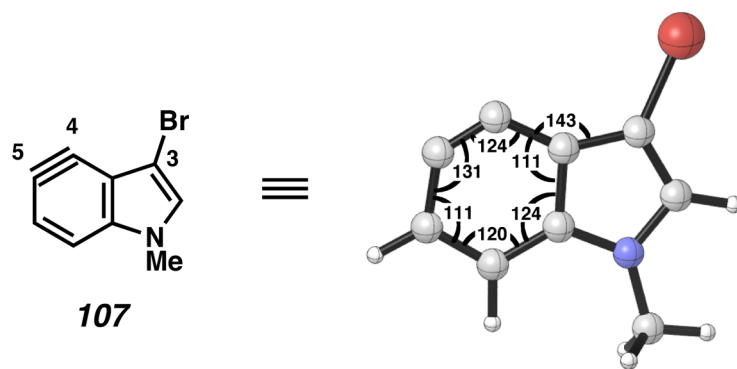
**Figure 10.** Distortion model for regioselective nucleophilic addition to fused arynes (X = electron-withdrawing group). The effect of X is larger than the more remote X'.



**Figure 11.** Internal angles for unsymmetrical arynes obtained from B3LYP/6-31G(d) optimized geometries.

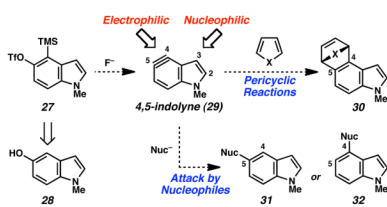


**Figure 12.** Internal angles for 4,5-, 5,6-, and 6,7-indolynes with varying *N*-substituents from B3LYP/6-31G(d) optimized geometries.

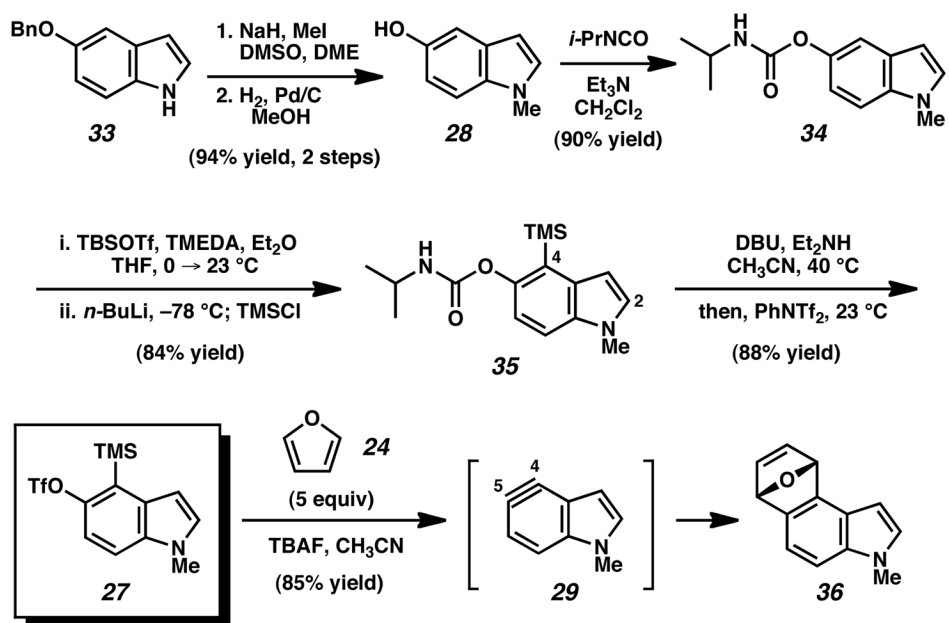


**Figure 13.**  
3-bromo-4,5-indolyne **107** and B3LYP/6-31G(d) optimized geometry.

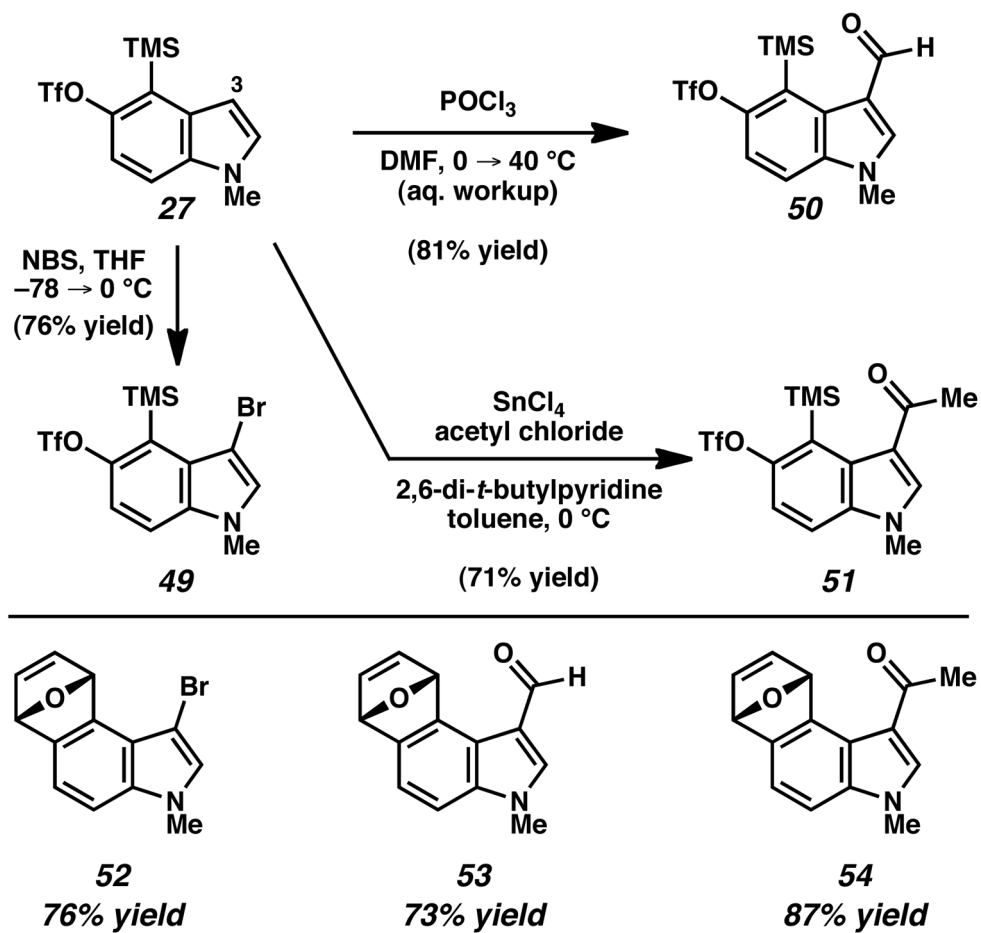




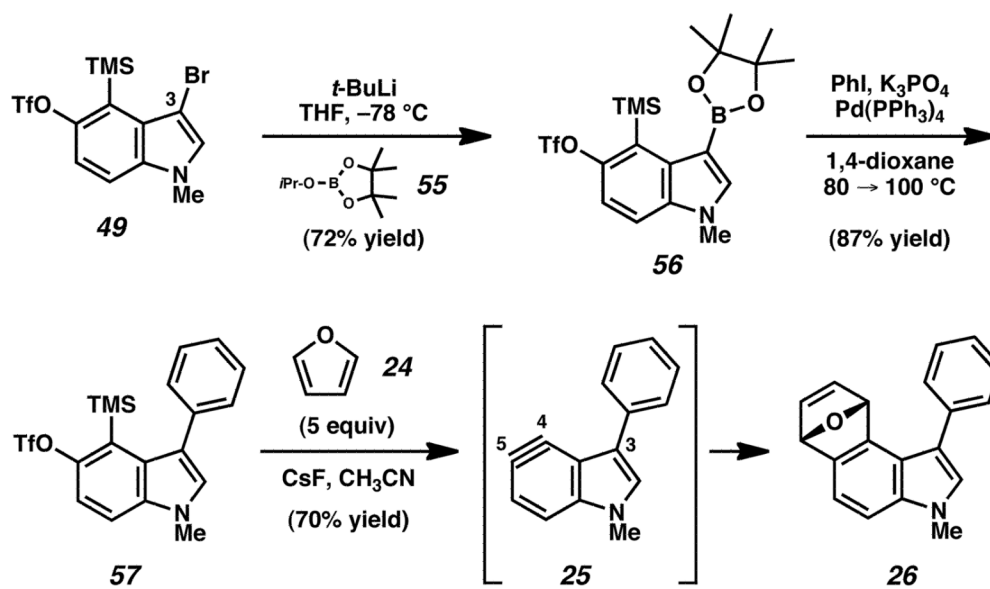
Scheme 1.



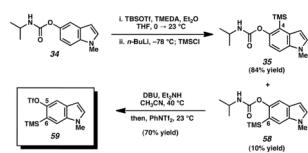
Scheme 2.



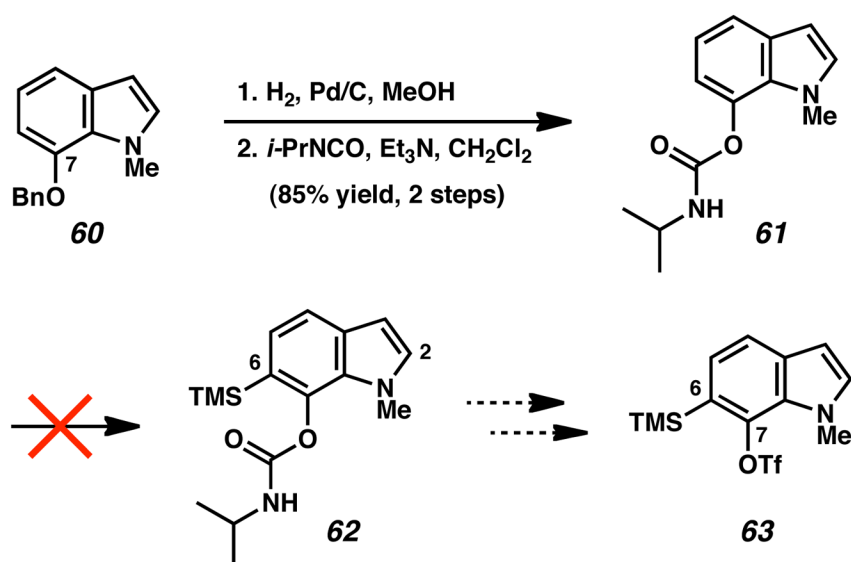
Scheme 3.



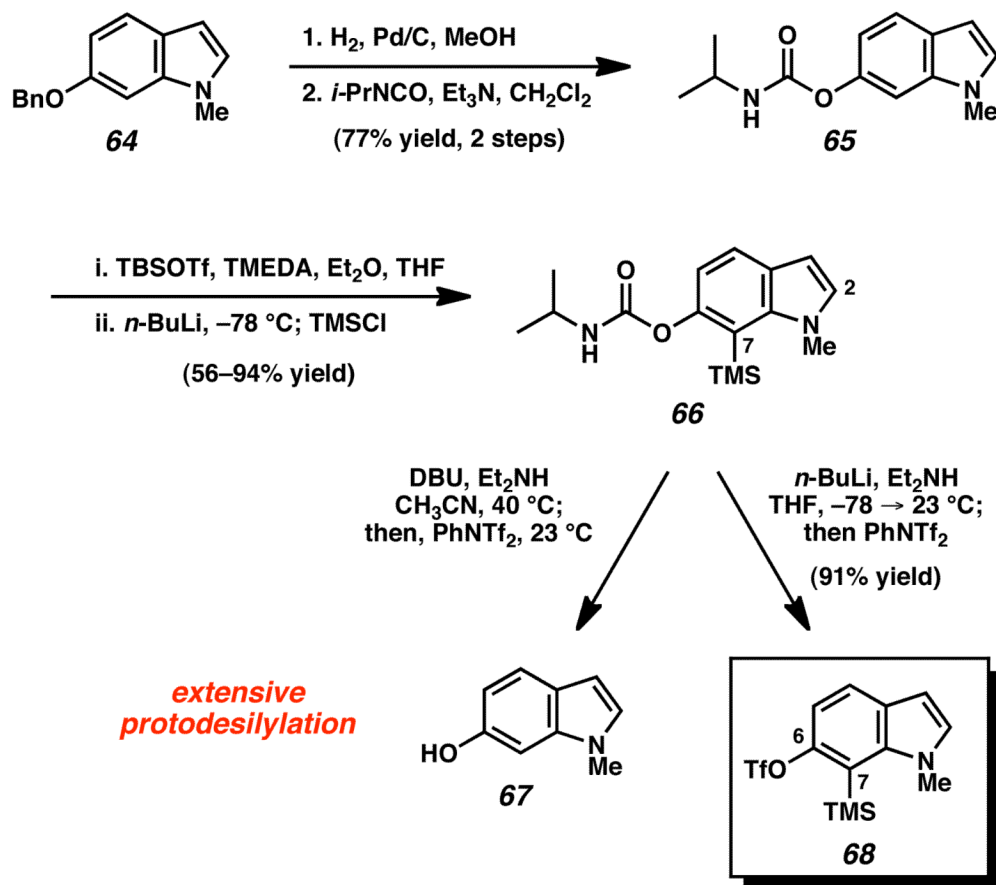
Scheme 4.



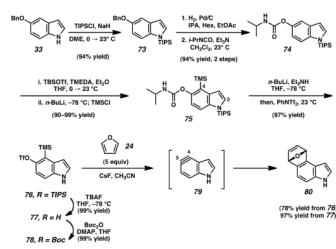
Scheme 5.



Scheme 6.

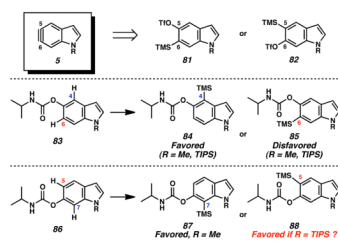


Scheme 7.

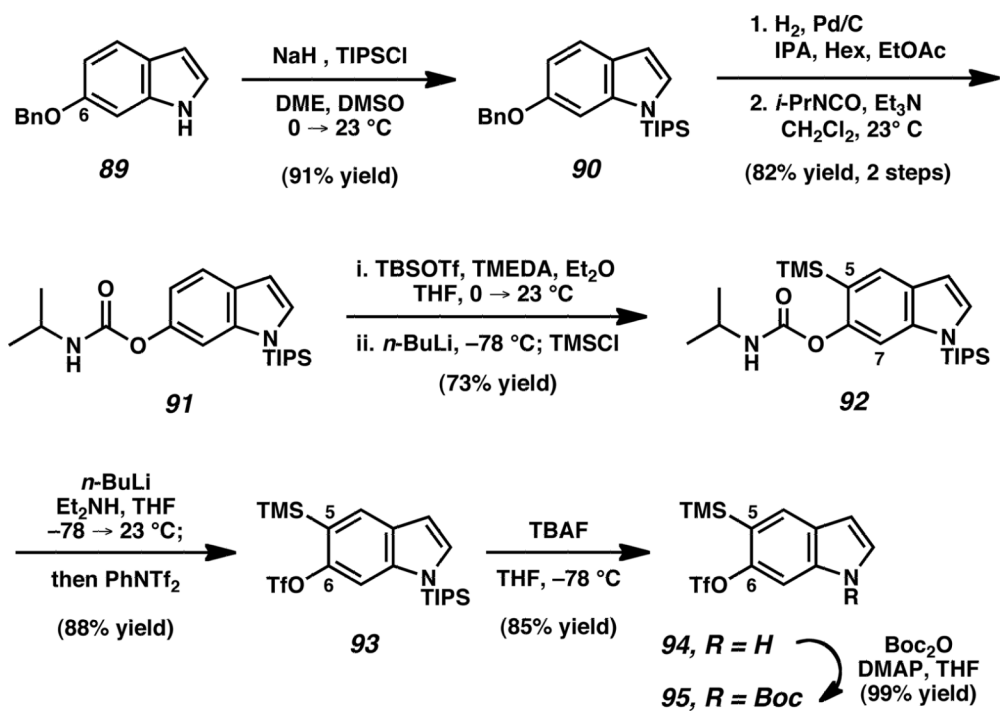


Scheme 8.

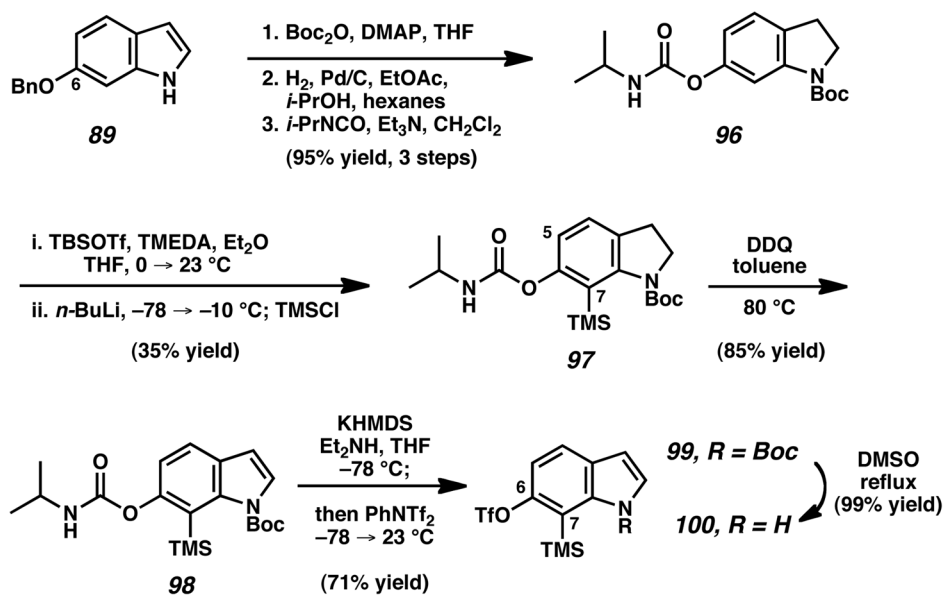




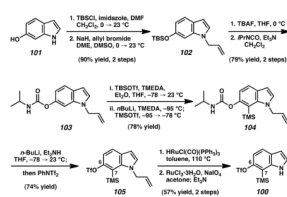
Scheme 9.



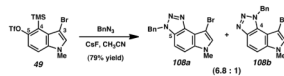
Scheme 10.



Scheme 11.



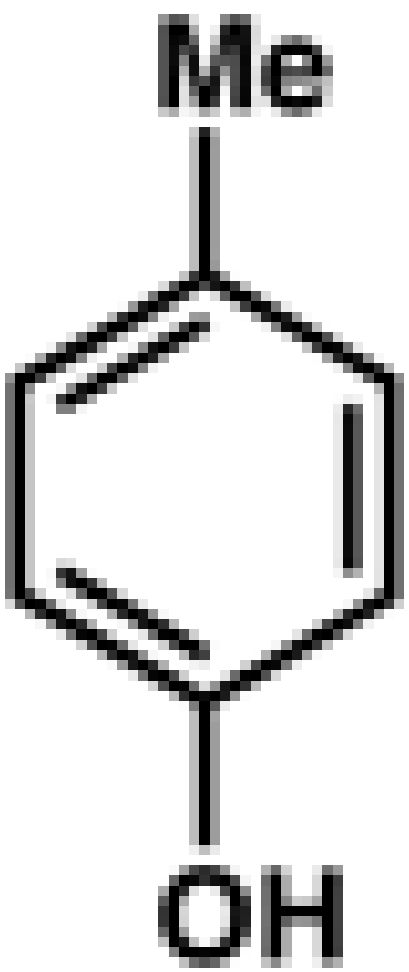
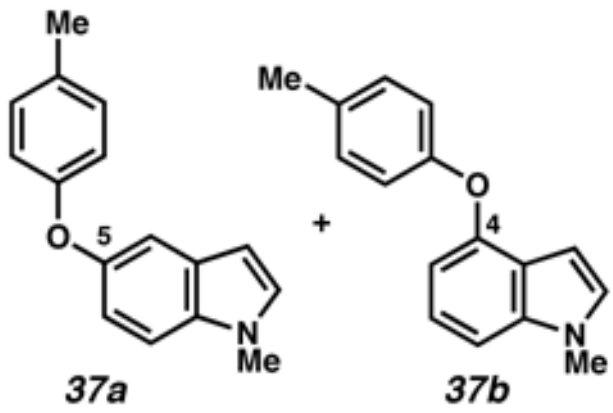
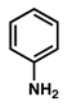
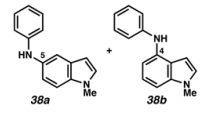
Scheme 12.

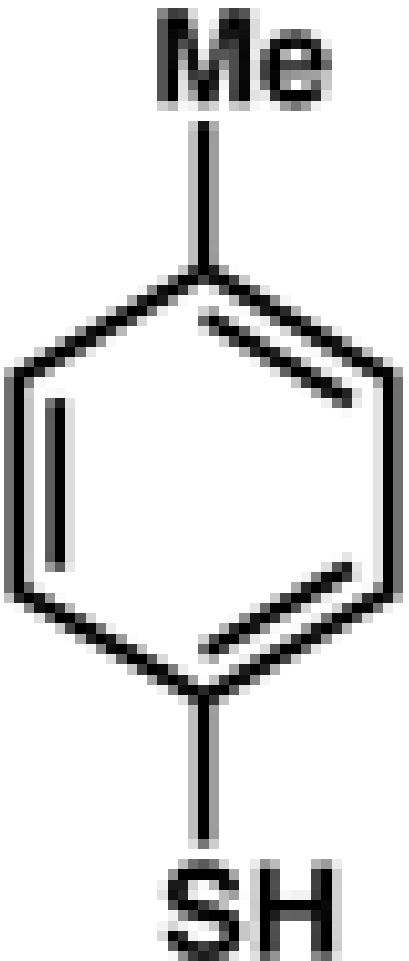
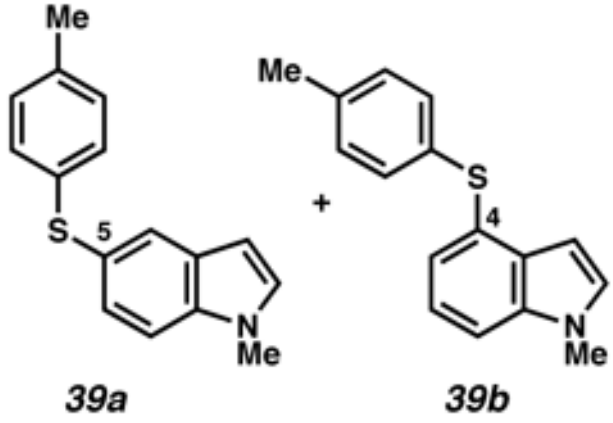
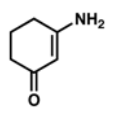
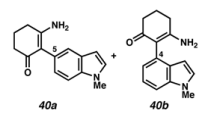
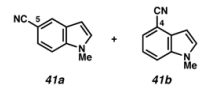


Scheme 13.

Table 1

Nucleophilic additions to 4,5-indolyne **29**

entry	trapping agent	products	yield (ratio)
1 <sup>a</sup>			80% yield (3:1)
2 <sup>a</sup>			91% yield (12.5:1)

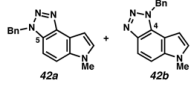
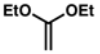
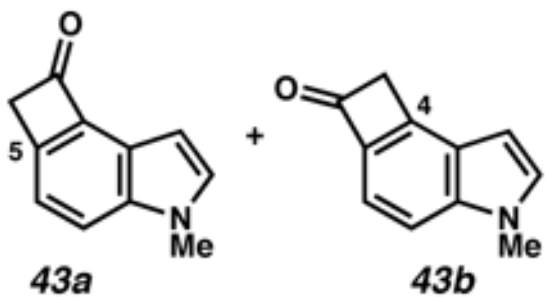
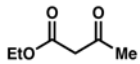
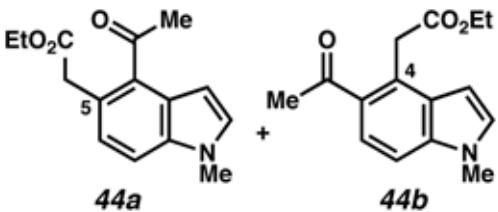
entry	trapping agent	products	yield (ratio)
3 <sup>a</sup>			88% yield (2:1)
4 <sup>b</sup>			58% yield (10:1)
5 <sup>a</sup>	KCN		85% yield (3.3:1)

<sup>a</sup> Conditions: **27**, CsF, CH<sub>3</sub>CN, 50 °C.

<sup>b</sup> Conditions: **27**, CsF, CH<sub>3</sub>CN, 40 °C.

Table 2

Formal cycloaddition reactions of 4,5-indolyne **29**

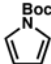
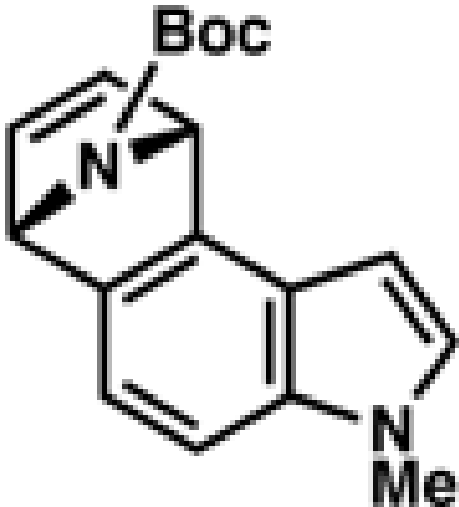
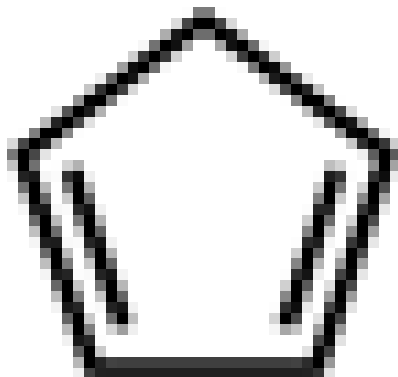
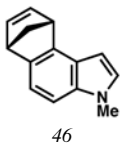
entry	trapping agent	products	yield (ratio)
1 <sup>a</sup>	N <sub>3</sub> -Bn		86% yield (2.4:1)
2 <sup>b</sup>			86% yield (5.5:1)
3 <sup>c</sup>			68% yield (2:1)

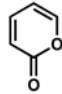
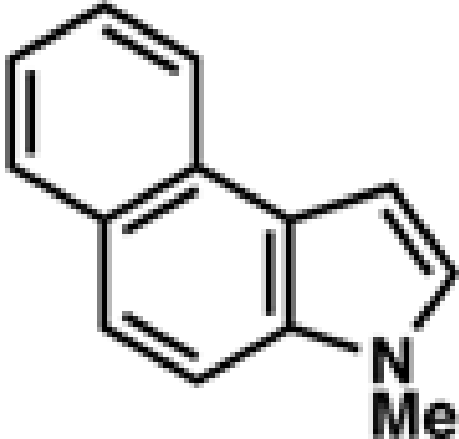
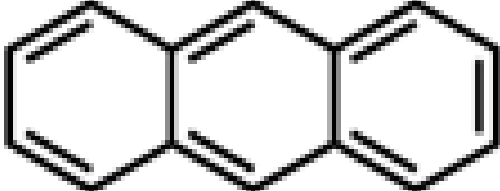
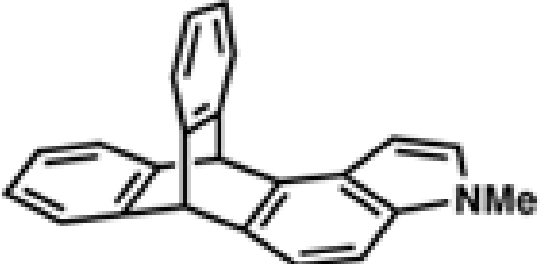
<sup>a</sup> Conditions: **27**, TBAF, CH<sub>3</sub>CN, 23 °C.<sup>b</sup> Conditions: **27**, CsF, CH<sub>3</sub>CN, 23 °C.<sup>c</sup> Conditions: **27**, CsF, CH<sub>3</sub>CN, 80 °C.



Table 3

Diels–Alder reactions of 4,5-indolyne **29**

entry	trapping agent	product	yield
1 <sup>a</sup>			83% yield
2 <sup>a</sup>			65% yield

entry	trapping agent	product	yield
3 <sup>b</sup>		 47	85% yield
4 <sup>c</sup>		 48	72% yield

<sup>a</sup> Conditions: **27**, TBAF, CH<sub>3</sub>CN, 23 °C.

<sup>b</sup> Conditions: **27**, CsF, CH<sub>3</sub>CN, 100 °C.

<sup>c</sup> Conditions: **27**, CsF, CH<sub>3</sub>CN, 80 °C.

Table 4

Nucleophilic additions to 4,5-indolyne **29**<sup>a</sup>

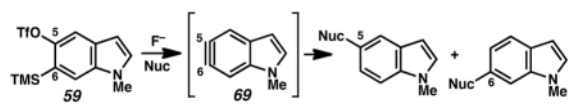
The reaction scheme shows the conversion of compound **27** (a 4,5-indolyne derivative with TMS and TIO groups) to intermediate **29** (a 4,5-indolyne derivative with a methyl group) using F<sup>-</sup>. Intermediate **29** then reacts with a nucleophile (Nuc) to form two regioisomeric products: Nuc-5 and Nuc-4.

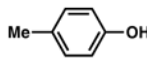
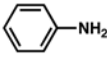
trapping agent (Nuc)	yield (ratio)	(computed)
	80% (3 : 1)	$\Delta\Delta G^\ddagger = 2.8$ (115 : 1)
	91% (12.5 : 1)	$\Delta\Delta G^\ddagger = 3.0$ (160 : 1)
N <sub>3</sub> -Bn	86% (2.4 : 1)	$\Delta\Delta G^\ddagger = 0.6$ (2.5 : 1)
KCN	85% (3.3 : 1)	C-5 preferred <sup>b</sup>

<sup>a</sup> Conditions: see supporting information. Computed ratios obtained from Boltzmann factors using B3LYP/6-31G(d) free energies including CPCM solvation by MeCN.

<sup>b</sup> Attack at C5 is favored (see SI).

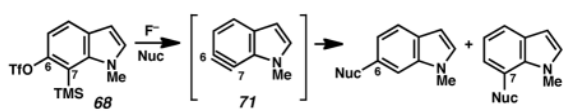
Table 5

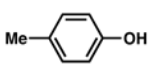
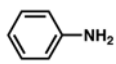
Nucleophilic additions to *N*-Me-5,6-indolyne<sup>a</sup>


trapping agent (Nuc)	yield (ratio)	(computed)
	64% (2 : 1)	$\Delta\Delta G^\ddagger = 1.7$ (18 : 1)
	73% (3 : 1)	$\Delta\Delta G^\ddagger = 0.7$ (3.3 : 1)
N <sub>3</sub> -Bn	94% (1.6 : 1)	$\Delta\Delta G^\ddagger = 0.4$ (1.8 : 1)
KCN	84% (1.7 : 1)	C-5 preferred <sup>b</sup>

<sup>a</sup> Conditions: see supporting information.<sup>b</sup> Attack at C5 is favored.

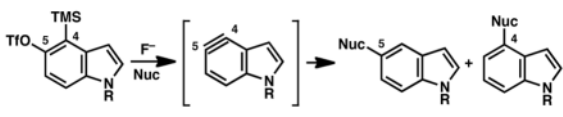
Table 6

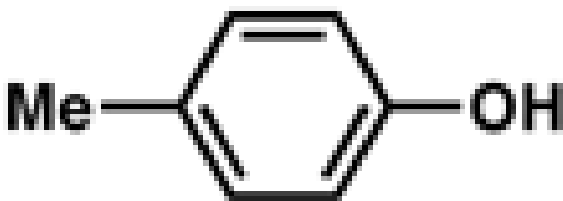
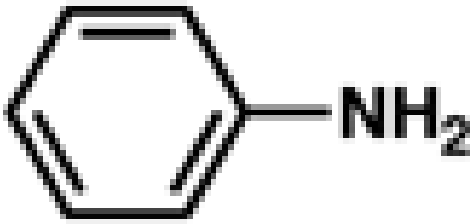
Nucleophilic additions to 6,7-indolyne **71**<sup>a</sup>


trapping agent (Nuc)	yield (ratio)	(computed)
	53% (C7 not observed)	$\Delta\Delta G^\ddagger = 11.4$ (solely C6)
	91% (C7 not observed)	$\Delta\Delta G^\ddagger = 5.5^b$ (solely C6)
N <sub>3</sub> -Bn	77% (C7 not observed)	$\Delta\Delta G^\ddagger = 2.7$ (63 : 1)
KCN	70% (C7 not observed)	C6 preferred <sup>c</sup>

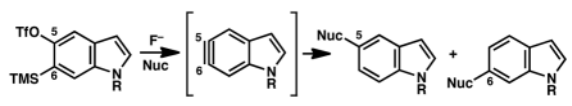
<sup>a</sup> Conditions: see supporting information.<sup>b</sup> C6 attack has no energetic barrier; C7 attack has  $\Delta\Delta H^\ddagger = 5.5$ .<sup>c</sup> Attack at C6 is favored (see supporting information).

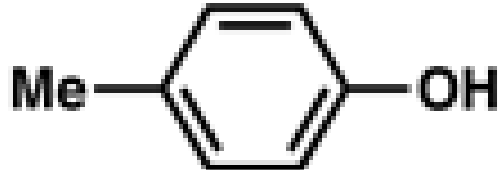
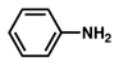
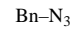

Table 7

Nucleophilic additions to 4,5-indolynes with varying *N*-substituents<sup>a</sup>


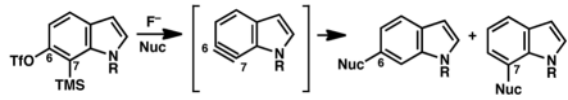
trapping agent (Nuc)	<i>N</i> -substituent (R)	yield	ratio (C5:C4)
	Me	80%	3 : 1
	H	67%	5 : 1
	Boc	68%	8.2 : 1
	Me	91%	12.5 : 1
	H	93%	6.4 : 1
	Boc	84%	8.3 : 1
Bn-N <sub>3</sub>	Me	86%	2.4 : 1
	H	75%	1.7 : 1
	Boc	78%	5 : 1
KCN	Me	85%	3.3 : 1
	H	67% <sup>b</sup>	3.4 : 1
	Boc	78%	3.5 : 1

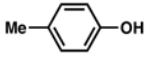
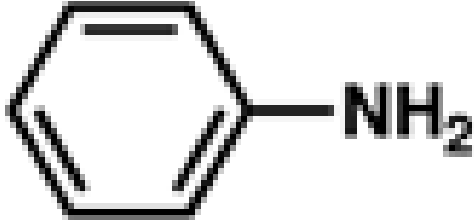
<sup>a</sup> Conditions: see supporting information.<sup>b</sup> Yield reported after Boc-protection

**Table 8**Nucleophilic additions to 5,6-indolynes with varying *N*-substituents<sup>a</sup>


trapping agent (Nuc)	<i>N</i> -substituent (R)	yield	ratio (C5 : C6)
	Me	64%	2 : 1
	H	72%	2 : 1
	Boc	72%	1.1 : 1
	Me	73%	3 : 1
	H	91%	2.9 : 1
	Boc	83%	1.5 : 1
	Me	94%	1.6 : 1
	H	90%	1.8 : 1
	Boc	82%	1.3 : 1
	Me	84%	1.7 : 1
	H	40% <sup>b</sup>	1.8 : 1
	Boc	67%	1.6 : 1

<sup>a</sup>Conditions: see supporting information.<sup>b</sup>Yield reported after Boc-protection

**Table 9**Nucleophilic additions to 6,7-indolynes with varying *N*-substituents<sup>a</sup>


trapping agent (Nuc)	<i>N</i> -substituent (R)	yield	ratio (C6 : C7)	
	Me	53%	C6 only	
	H	52%	10.7 : 1	
	Boc	59%	C6 only	
	Me	91%	C6 only	
	H	79%	13.8 : 1	
	Boc	66%	C6 only	
	Me	77%	C6 only	
	H	60%	6.9 : 1	
	Boc	63%	C6 only	
	Me	70%	C6 only	
	KCN	H	44%	7.6 : 1
	Boc	80%	C6 only	

<sup>a</sup>Conditions: see supporting information.